J.A. Reggia, E. Ruppin and D. Glanzman (Eds.)
Progress in Brain Research, Vol 121

CHAPTER 12

Unmasking unmasked: neural dynamics following stroke

William W. Lytton*, Samuel T. Williams and Samuel J. Sober

Department of Neurology, Neuroscience Program, University of Wisconsin, Wm. S. Middleton VA Hospital, 1300 University Avenue, MSC 1715, Madison, WI 53706-1532, USA

Anatomy is not destiny

Recovery from disease involves the interaction of the biological substrate with behavior. Nowhere is this more clearly seen than in the setting of a neurological disease such as stroke, where mind and behavior are directly, though sometimes subtly, affected. During recovery from stroke, a large web of causal chains lead to an improved condition or to continued disability. Recovery starts with the mental and physical process of rehabilitation therapy, which alters the physical state of the brain as it teaches new strategies and enhances muscle tone. Subsequently, the altered brain patterns in part determine what further rehabilitative actions the patient is capable of, leading to a vicious or virtuous cycle. Although many aspects of these healing cycles are beyond our control and will likely remain so, there are points at which we can intervene. In order to achieve the greatest rehabilitative effect, we can choose the timing and type of rehabilitation strategy and pharmacotherapeutic measures that will produce desirable brain changes.

The difficulty in connecting brain and behavior is a prominent part of the more general problem of causality in neuroscience. Assigning cause is difficult because of the enormous complexity of this organ. Like the better understood liver or lung, the brain is studied using a variety of techniques that necessarily focus on only one aspect of that organ, whether molecular, anatomical, biophysical or physiological. In the case of liver or lung, however, it is not unusual to be able to explain some global function singly, with a molecular, cellular, or anatomical explanation. In the brain, however, anatomy is not destiny, nor is molecular biology destiny. Complex interactions among different levels of organization are responsible for the remarkable functionality of the brain.

In the dynamics of a cortical map, there are two major levels of operation. Cellular interactions depend on both anatomical connectivity and on the dynamics of physiology. While neural activation happens very quickly, in the order of milliseconds, activity-dependent synaptic reorganization occurs over hours or days. Though occurring on vastly different timescales, these two mechanisms interact. Synaptic change will occur on the basis of coincident neural activation, and neural activation will be determined by the underlying anatomical connections.

In order to determine how the adult brain compensates when damage occurs, we study the interactions among structure, physiology, and behavior. Recovery involves plasticity, hence anatomical change; the anatomical factors cannot be understood without reference to physiology and behavior. It should also not be understood without reference to the underlying molecular receptor level, since these receptors will be the target of pharmacotherapeutic intervention in the recovery process. The goal of computer modeling in our

*Corresponding author. Tel.: (608) 265 3524; Fax: (608) 262 2327; e-mail: bill//@neurosim.wisc.edu

studies is to understand the interaction among levels of organization, as cells determine networks and networks behavior (Sejnowski et al., 1988). These interactions are not unidirectional; anatomy determines physiology, which determines behavior, but behavior also determines physiology, which determines anatomy.

Plasticity in the adult brain

The goal of our research is to discover and take advantage of causal links that help or hinder recovery from stroke. To this end, we must devise a model that can account for what is seen in the physiology of animals and patients, and the changes they undergo before and after stroke. Models give us a quantifiable way to evaluate qualitative hypotheses concerning the mechanisms underlying physiological changes observed experimentally. They also suggest new hypotheses through the emergence of unexpected and unintended consequences. In the end, such models will lead to a deeper understanding of the processes of adult plasticity, suggesting better rehabilitation techniques for those suffering from impaired function.

Cortical damage is often the result of cerebrovascular accident, which leads to the death of neural tissue. The vascular system has an organization and structure that is largely independent of the underlying brain regions. Since blood vessels are superimposed onto the nervous system, damage to the vessels affects parts of several functional neural areas rather than a single functional area in its entirety. Because of this, pure cases of single-region damage are very rare, and the majority of strokes lead to deficits in many tasks. To recover function, the remaining neural tissue must demonstrate plasticity.

Plasticity in the youthful brain has been well demonstrated, but our understanding of adult mechanisms is still lacking. The studies of Hubel and Wiesel firmly established the concept of a critical period in early brain development (Hubel, 1996; Hubel and Wiesel, 1998). Studies have shown that the establishment of ocular dominance, the ability to detect edges, and general cortical mappings, can be established only during a critical developmental stage (Miller, 1995). Such research suggested that primary cortical organization is, for the most part, fixed from an early age. Of course, adult cortex is remodeling all the time, learning new memories and abilities. Recent studies of somatosensory and visual areas have also demonstrated adult plasticity at the cellular level. However, fundamental change is probably seldom called for outside of the domain of ablative diseases such as stroke (Nudo et al., 1996).

The existence of plasticity in the adult brain has been primarily demonstrated in three ways: peripheral manipulation, intracortical microstimulation, and animal models of stroke. Most of these studies rely on the alteration of stimulus characteristics; for example, the removal of a finger or the presence of constant stimulation (Merzenich and Kaas, 1982; Wang et al., 1995; Buonomano and Merzenich, 1998). In general, cortical reorganization will occur so that heavily stimulated areas will see an increase in the size of their cortical maps, and weakly stimulated areas will see a reduction in representation (Clark et al., 1988; Robertson and Irvine, 1989; Kaas et al., 1990; Allard et al., 1991; Gilbert and Wiesel, 1992; Weinberger et al., 1993). Intracortical microstimulation shows another form of plasticity, in which stimulation of a cortical site will cause neurons in the vicinity to have receptive fields similar to the stimulated neurons (Dinse et al., 1990; Nudo et al., 1990; Smits et al., 1991; Recanzone et al., 1992). In animal models of stroke, the receptive fields of surviving cells expand, contract, and shift so as to occupy the space previously covered by the dead cells (Yamasaki and Wurtz, 1991; Alamancos and Borrel, 1995; Sober et al., 1997; Lytton et al., 1999).

The basic model

Computational studies have assumed that recovery from cortical damage, recovery from peripheral damage, or response to a change in stimulus pattern of any kind would occur in two phases that correspond to the vastly different time constants of neural response and synaptic plasticity. This assumption has been partially confirmed by studies of long-term potentiation, occurring over a timeframe several orders of magnitude greater than that

of neural activation. Animal studies suggest that behavioral recovery may take place in two or more phases, consistent with this assumption (Nudo et al., 1996; Nudo and Milliken, 1996). According to the basic computational model, these two phases can be grossly characterized as: (1) dynamics; and (2) plasticity (Armentrout et al., 1994; Goodall et al., 1997). In the dynamic phase, changes in cell activity are due to the alteration in inputs to the remaining cells following an ablation. In the plastic phase, these alterations in cell activity start to change synaptic strengths, presumably through a Hebbian process relating strength increases to paired presynaptic and postsynaptic activity.

The middle temporal visual area (area MT) has neurons that respond to visual motion. Thus, these cells do not respond to stationary stimuli but do respond when something moves in the visual field. Like cells in other visual areas, these cells have retinotopic tuning, that is, an individual cell will respond to a stimulus in one area of the visual field but will not respond to stimuli in other areas. Unlike cells in other visual areas, which may also be tuned to stimulus orientation or color, these cells are tuned to the attributes of visual motion: speed and direction. Small ablations of area MT lead to changes in the receptive fields of neighboring, non-ablated cells and to changes in the ability of an animal to perceive motion (Wurtz et al., 1990; Yamasaki and Wurtz, 1991).

In order to construct simple computer models of cortical dynamics, it is useful to generalize the concepts of receptive field and projective field (Fig. 1). Experimentally, a receptive field is the set of stimuli that will activate a particular neuron. In visual area MT, this receptive field includes both the retinotopic receptive field and the receptive field for speed and direction. In a sensory system, the projective field does not always have a clear operational definition. Ideally, the projective field of an elemental stimulus would correspond to the set of neurons activated. However, it is not generally possible to define an elemental stimulus nor to measure from multiple cells in order to determine which ones have been activated.

Our basic neural network model for exploring receptive fields consists of input and processing layers (Fig. 1, see Appendix for details) (Miller et al., 1989; Miller, 1994). The many layers of brain that lie between photoreceptor and high-order cortical area are collapsed into these two layers. Because of this foreshortening, the input layer is alternately conceived of as a primary receptor array for the purpose of mapping receptive fields, or as a thalamic or lower-level cortical area for the purpose of assessing cellular interactions. In our simulations we consider the input layer to be V1 (primary visual area) and the main processing layer to be area MT. The V1 layer is simply a set of input values and not a set of processing units. Each cell in the MT layer receives stimulation from many cells in the V1 layer. This convergence can be regarded as an 'anatomical receptive field'. Correspondingly, the divergence from a single V1 layer unit to a set of MT units can be regarded as an 'anatomical projective field'. The physiological responses of individual neurons in the network are not fully determined by these feedforward projections from V1 to MT, however. Within the MT layer, there are lateral connections which provide proximal excitation and more distant inhibition in a center-surround or 'Mexican hat' pattern (Fig. 1(B)). Activity mediated through these connections will interact with feedforward activity to produce excitation of the MT units. Because of the complexity of these interactions, it is not possible to determine the activity patterns by reference to the connectivity alone. Instead we must run simulations, analogs of physiological experiments, in order to measure receptive fields by mapping all stimulus locations that will produce suprathreshold responses in a specified MT cell.

Receptive field changes following ablation

Physiologically, receptive field expansion and receptive field contraction are both observed in the surrounding cells that remain alive following an ablation (Fig. 2(A,C)). Technically, it is not possible to sample the same cell both pre- and postablation. Therefore, it is not possible to say whether a receptive field of a particular cell has become larger or smaller. One can however, sample a large number of cells in the same area both before and after the ablation. Postablation receptive fields were in many cases substantially larger than any of

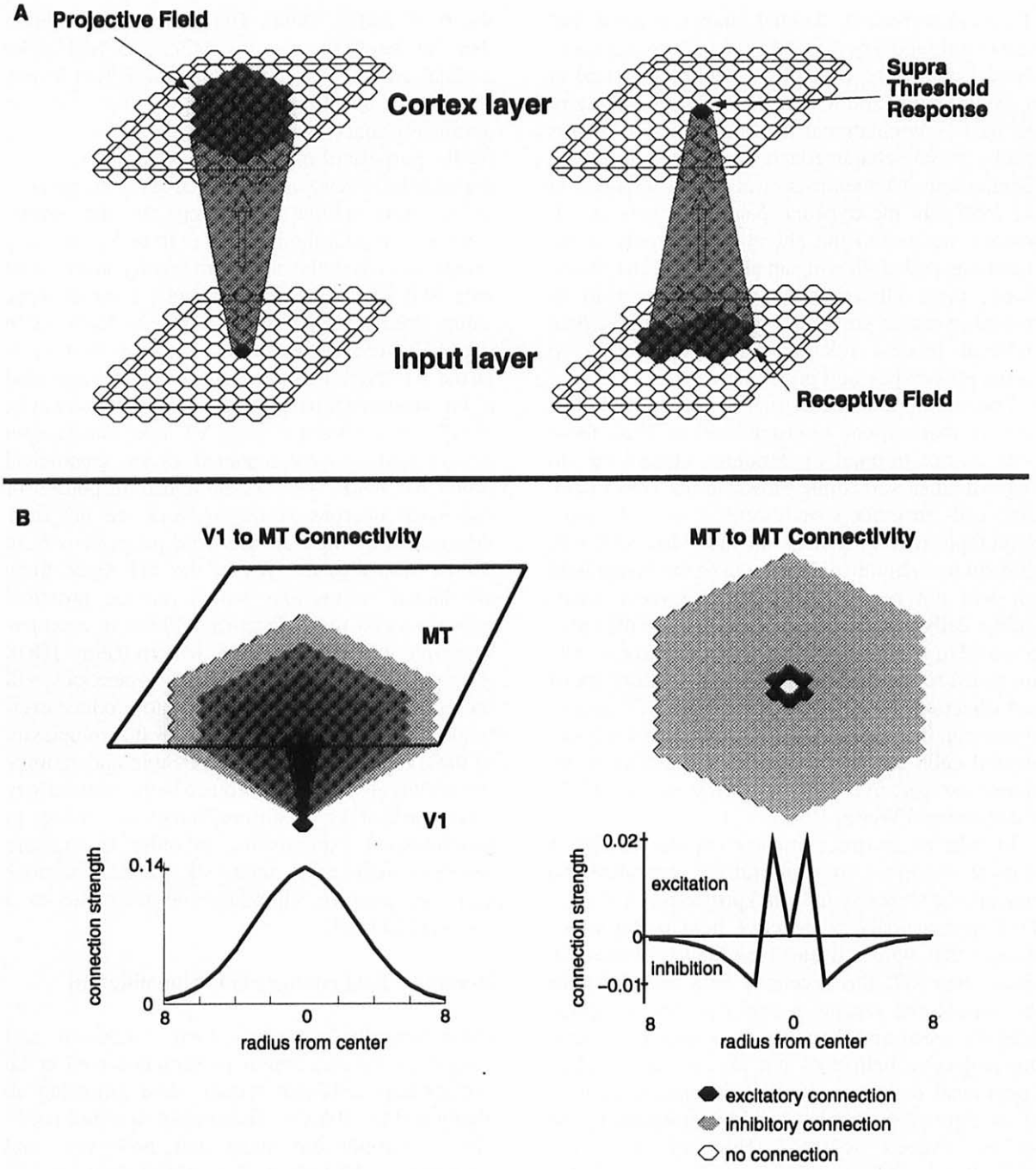

Fig. 1. (A) Computer model schematic: input layer (V1) and output layer (MT) are both two dimensional hexagonally tesselated arrays of nodes. Projective fields (left) are defined by the spread of activity to nodes in the output layer following stimulation of a single node in the input layer. Receptive fields (right) are defined by units in the input layer that can stimulate a given output unit layer to a supra threshold response. (B) The strength of connections from input to output layer (left) falls off according to a Gaussian function of lateral distance. Lateral connectivity in the output layer is also non-uniform (right). The region surrounding the excited unit is laterally excited by the central node, but nodes further away are inhibited. The result is a 'Mexican hat' (sombrero-shaped) pattern of connection weights.

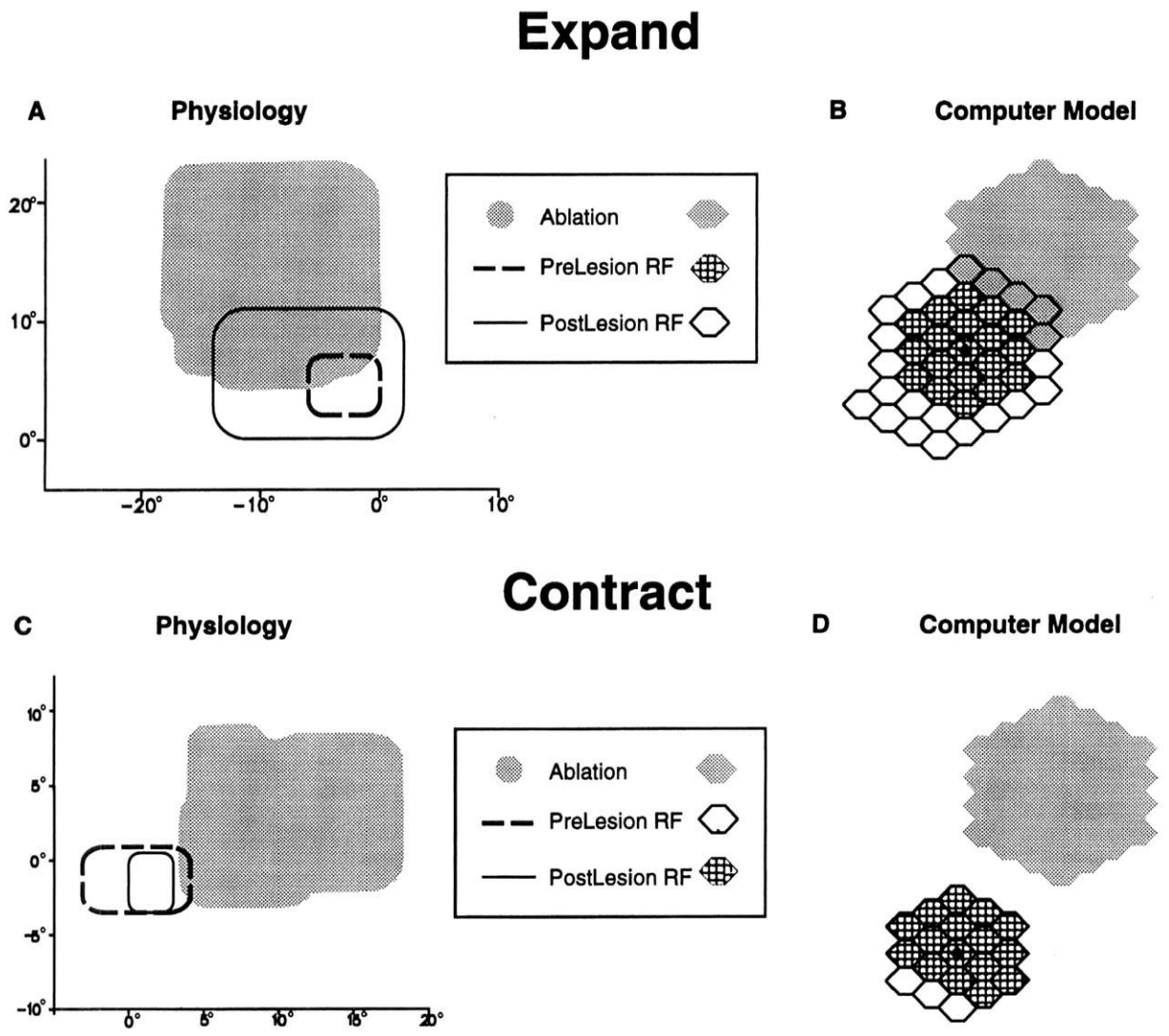

Fig. 2. (A) Receptive field (RF) expansion following ablation in visual area MT of macaque. The pre-lesion receptive area in V1 (dashed line) expands after the ablation (grey) in the MT layer. RFs are represented in degrees of visual space. Adapted from Sober et al. 1997, Fig. 2. (B) Postlesion expansion in the computer model. Before the lesion, the model shows a uniform RF in V1 around the MT unit, (hash marks). After the lesion, the altered MT activation dynamics close to the lesion yield an increase in RF size (hexagons). (C) RF contraction following ablation in visual area MT of macaque. The pre-lesion receptive area in V1 (dashed line) expands after the ablation (grey) in the MT layer. Adapted from Sober et al. 1997, Fig. 3. (D) The computer model of RF contraction also shows postlesion contractions. Again, the prelesion RF (hexagons) is uniform. After the lesion, the RF contracts (hash marks).

those seen before the lesion, suggesting that there had been receptive field expansion in many cells. Often this expansion was asymmetrical with a tendency to expand more in the direction of the lesion. Other postablation receptive fields were noted to be smaller than any seen preablation, suggesting that others had contracted. These expansions and contractions were the basic data we sought to explain using the computer model.

The basic model could easily produce expansion of receptive fields (Fig. 2(B)). This is the phenomenon of unmasking, the revealing of connections

whose functional consequences were previously not apparent due to coincident inhibition. Expansion occurred because even weak divergent input from the input layer could now excite units that were previously inhibited disynaptically by the cells within the lesion area. Unmasking made the physiological receptive field correspond more closely to the anatomical receptive field. Therefore, the maximum extent of unmasking was determined by the width of convergence from the input layer. In general, greater convergence allowed more receptive field expansion, hence more unmasking. In this initial model, expansions were relatively modest, far less than what the divergence from the input layer could permit. The model also produced receptive field contraction; these were also not very substantial (Fig. 2(D)).

The computer model explains these receptive field changes

In the premorbid state (before the lesion), the cells that will be ablated provided near excitatory inputs and far inhibitory inputs. After the ablation these influences were lost and this produced the sequence of effects that resulted in the expansion and contraction observed in the model (Fig. 3). The primary effect of lesion in our model was a loss of local excitatory and distal inhibitory connections originating from the ablated region. The excitatory influence was only nearest neighbor, so the majority of excitatory connections within the lesion targeted other ablated cells and their loss had little effect on the surrounding regions. The loss of the inhibitory connections, with their much greater divergence, produced disinhibition in the ablation surround, resulting in increased excitability of cells outside the lesion, with the effect decreasing with distance. This increased excitability led to increases in receptive field size, for inputs previously unable to yield a suprathreshold response now had less inhibition to counter. Expansion and contraction in the basic model represented an expanding wave of consequences from the loss of projections that had emerged from the lost neurons. The divergent excitatory stimulus from the input layer remained unchanged but the lateral forces were diminished resulting in an imbalance that was rectified through a shift in responses until a new steady-state is reached. (These models always reached a steady

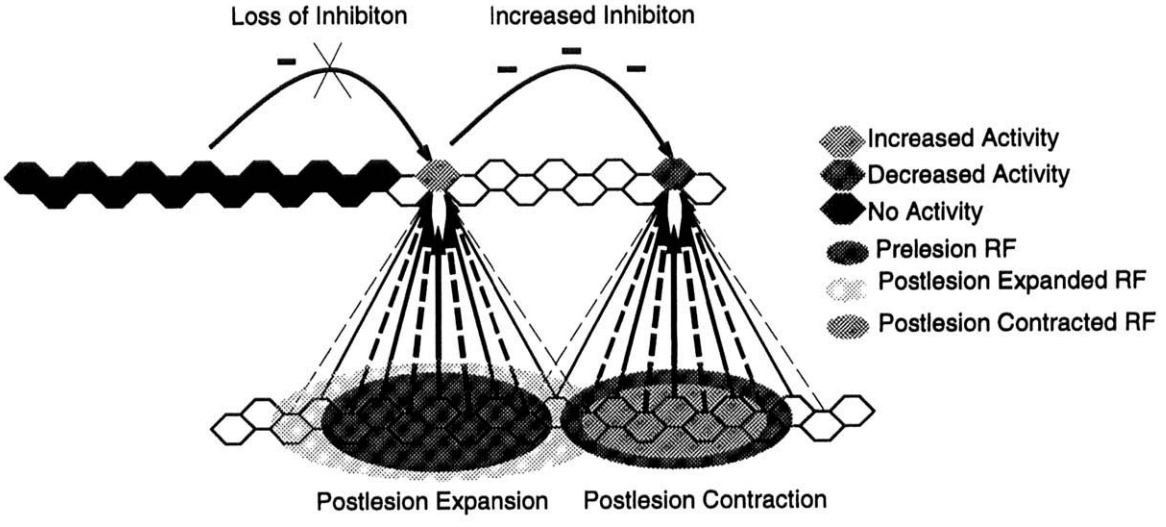

Fig. 3. Schematic explanation of postlesion expansion (left) and contraction (right). A loss of inhibition from ablated regions in the cortex (black hexagons), lead to an increase in activity of MT units close to the ablation (light grey hexagon) over the premorbid state. Inputs from V1 which were not able to yield a supra-threshold response (left light grey lines) are now part of the node's receptive field (left light grey oval). The highly activated MT unit (light grey hexagon), causes greater inhibition on units farther away from the ablation (dark grey hexagon) as a secondary effect. The receptive field for these units will decrease in size, for only strong connections from V1 (thick lines) will yield a supra-threshold response.

state in our simulations; in general a dynamic system could settle into oscillations or chaos instead.) The hunt for the new steady state could be viewed as a negotiation, as activated units influence other units and are influenced in turn.

The degree of disinhibition was not great enough to allow the weakest convergent feedforward projections to excite the MT unit. Although the degree of convergence (the size of the anatomical receptive field) is not an absolute limit for receptive field expansion, it is a practical limit. If inhibition is weak enough, then activity can spread laterally through the slice, allowing activation of MT units that do not receive any direct projections from V1. However, excessive lateral spread will lead to a hyperexcitable 'epileptic' network in which any stimulus will cause continuous activation of all cells.

The increased activity levels of units with expanded receptive fields had a secondary effect, increasing the inhibitory influence on other units within their ring of inhibitory projection (Fig. 1(B)). This generally led to decreased activity levels in these cells and made it more difficult for feedforward inputs from the input layer to excite them to threshold. Contraction in the basic model was thus a secondary consequence of the increased excitability of the units which showed receptive field expansion. Because sets of cells near and far from the ablation are mutually inhibitory, the reduction in activity of the far cells reduced their inhibitory effect on the near cells, allowing these to become still more active and produce greater inhibition in return. This effect of mutual inhibition can lead to a winner-take-all situation, in which one cell completely overwhelms the other. This does not occur here due to the continuing activation from the input layer.

Although the model did produce the basic effects of expansion and contraction, the contractions seen were minimal, leading us to miss them on our first set of simulations. We therefore explored other explanations for receptive field contraction, reconsidering our assumptions. Such reconsideration is a major aspect of computer modeling, a field which enjoys the distinction of making a virtue of failure. In this case, the failure to replicate substantial receptive field contractions led us back to the lesion histology, where further examination showed a reduction in binding proteins associated with inhibitory neurons (Sober et al., 1997). This suggested that there might exist a functional disinhibitory halo, which would be expected to augment both expansion and contraction of receptive fields. This was confirmed in the model. The disinhibitory halo model showed both very large expansions (Fig. 4(A)), as well as more pronounced contractions (Fig. 4(B)). Expansion augmentation is particularly pronounced within the disinhibitory halo itself since these cells are almost entirely without inhibitory influence and are therefore excitable by the relatively weak stimulation coming from distantly converging inputs. Subsequently, the increased hyperactivity of these units produced increased inhibition in the inhibitory ring, allowing for the more pronounced contractions. Although the explanation for expansion and contraction is the same as seen in the basic model, the effect is substantially augmented by the further disinhibition (Fig. 5). As expected, overall activation tended to be greater with the elimination of inhibition. However, activation changes were surprisingly minor (Fig. 5(B)).

The spread of activity change associated with ablation need not stop with second order effects. Given sufficient divergence from the input layer, one would anticipate that the decreased excitability of the cells in the receptive field contraction zone might produce another area of receptive field expansion still further out. We have not yet explored this prediction in detail, but it suggests a way in which reversible cortical lesions with cooling or lidocaine might be used to allow rapid assessment of effective divergence by demonstration of a standing wave of alternating peaks and troughs of both activity and receptive field size.

Behavioral implications

Beyond the receptive field level of MT neural responses lies a level of processing that will take the information, determine what is being seen and act on the basis of that information (Oram et al., 1998). In essence this involves a decoding of information present in MT. We have not made an effort to model the details of neural processing

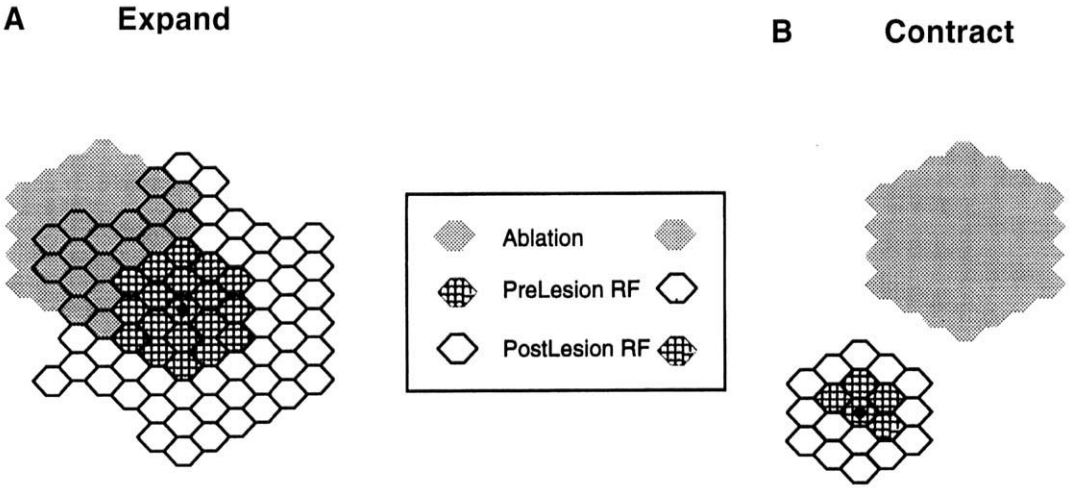

Fig. 4. (A) Receptive field (RF) expansion is more dramatic in the disinhibitory halo model, particularly for those excitatory neurons that lie in the disinhibitory halo itself. (B) RF contraction is also more pronounced in the disinhibitory halo model. The mechanism is the same as was seen in the simpler model but the increased activation of excitatory neurons in the disinhibitory halo causes a greater secondary inhibition more distally, producing greater contraction.

involved in this decoding. Nor do we wish to speculate as to the nature of conscious experience, but only to explore simple statistical methods that could be used to interpret the 'code' generated by the firing of cortical neurons that correspond to the external object. Another way of looking at this situation is in terms of Bayes' theorem, establishing the probability that the stimulus is moving in a certain direction based on the conditional probability of a particular set of cells firing in such a case and the overall probability distribution of cell firing and stimulus likelihood.

As noted above, dynamic alterations are the first of two major phases of response that depend on the

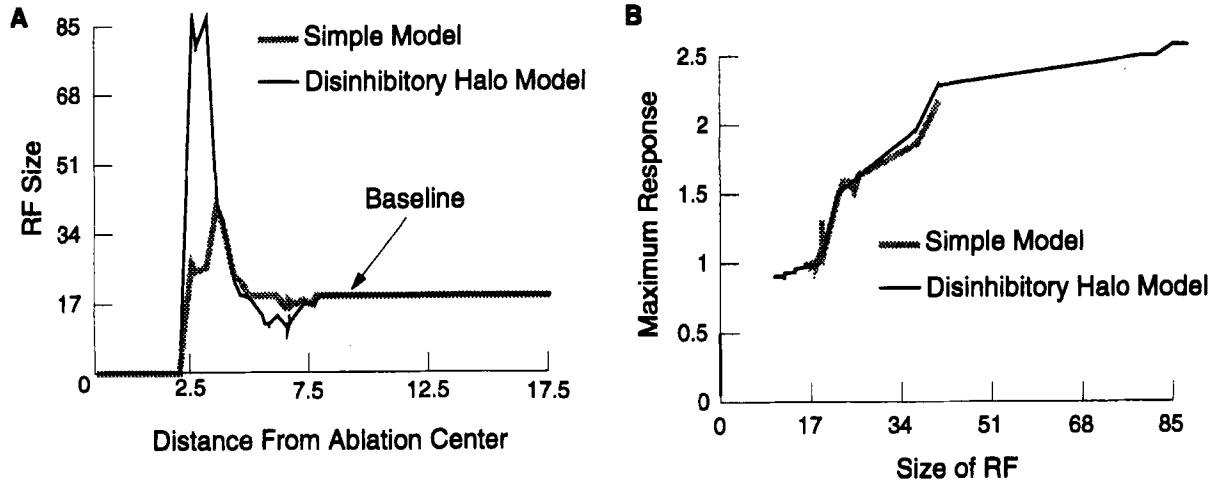

Fig. 5. (A) Both receptive field (RF) expansion and contraction are greater in the disinhibitory halo model. Cells within the ablation radius have receptive fields of size zero. (B) Despite the different MT connection weights in the basic and disinhibitory models, the level of activation relative to RF size were very similar. In both models, maximum activity of the cells was highly correlated with RF size. The main difference between models was that the disinhibitory model had cells achieving activation levels beyond what occurred in the basic model.

vastly differing time constants of neural dynamics and synaptic plasticity. Although we have not yet explored these true plastic changes, they have been explored by other authors (Grajski and Merzenich, 1990, 1990a; Xing and Gerstein, 1994; Sutton and Reggia, 1994; Goodall et al., 1997). In general, these authors have assumed that synaptic plasticity will follow some form of Hebbian algorithm, with increase in connection strength between simultaneously active cells and perhaps decreases between asynchronously active cells. There remains uncertainty as to whether plasticity is primarily confined to the feedforward projections from the input layer, to the intrinsic connections, or is present in both locations.

As a first approximation, the Hebbian algorithm simply serves to imprint firing relationships that are already present and would therefore not be expected to produce major alterations in receptive field morphology (Hebb, 1949). However, a variety of plastic processes occur in intermediate time frames (Fisher et al., 1997), suggesting that the dichotomy between dynamics and plasticity may not be clean. Furthermore, as noted above, the relation between dynamics and plasticity is not one way: dynamic change begats plasticity but plasticity is structural change that begats dynamic change.

This inner loop of dynamic/plastic interactions is embedded in an outer loop of behavioral/molecular interactions. A physical neurorehabilitative therapy acts at the behavioral level, presenting particular stimuli in a damaged sensory system or suggesting movement sequences to treat a disabled motor system. Simultaneously, molecular alterations are affected by pharmacological therapies. In order to begin to understand these interactions, we must consider how neural activity produces sensorimotor coordination, as well as how behavior alters neural activity.

Uncertainty regarding the locus of plasticity also arises when considering the behavioral level. We have shown that a stroke will involve alterations in receptive fields. Extending the statistical or coding viewpoint mentioned above, these changes represent an alteration in the encoding of the external stimulus. If the decoding strategy leading to behavior were to remain unchanged, function would suffer. For that reason, full behavioral recovery will require changes in decoding strategy that match the alterations in encoding. We have hypothesized that the immediate receptive field changes, manifestations of the disorder, are also the first steps towards recovery. Therefore, we expect that there will be an alteration in decoding strategy as well.

The original model, presented above, simply provided the location of the perceived object without identifying any of its other attributes (Fig. 1). Of course, visual areas also encode other stimulus attributes, such as color, shape or motion. In the case of visual area MT, the neurons are specialized to encode information about speed and direction of motion. In order to model the animal's calculation of speed and direction, it was necessary to model the response of individual neurons to these attributes.

We organized the inputs in order to get representations of location, speed and direction of an input stimulus (Fig. 6). To keep things as simple as possible, input was represented as a stimulus with attributes of location, direction of motion, and speed. Input was cosine-filtered in both the direction and speed domains. Similarly, each MT-layer unit in the original model was replaced with a set of units, each of which was assigned a preferred direction and speed. As in the original model, MT-layer units were connected to each other through a Mexican hat pattern of excitatory and inhibitory weights.

Behavior as a synthesis of neural activation

Following Georgopoulis and colleagues (1982, 1986), we chose to model the decoding of information by assuming that each MT neuron contributes to the representation of the stimulus by 'voting' for a vector, which corresponds to that neuron's preferred direction and speed. That is, firing in a particular MT cell is interpreted as a vote for the hypothesis that the stimulus is the neurons' preferred stimulus. We tested three basic algorithms for how the collected 'vector votes' of many MT units could be synthesized into a single representation of the stimulus: winner-take-all, vector average and vector sum. The winner-take-all algorithm is commonly used in artificial neural networks

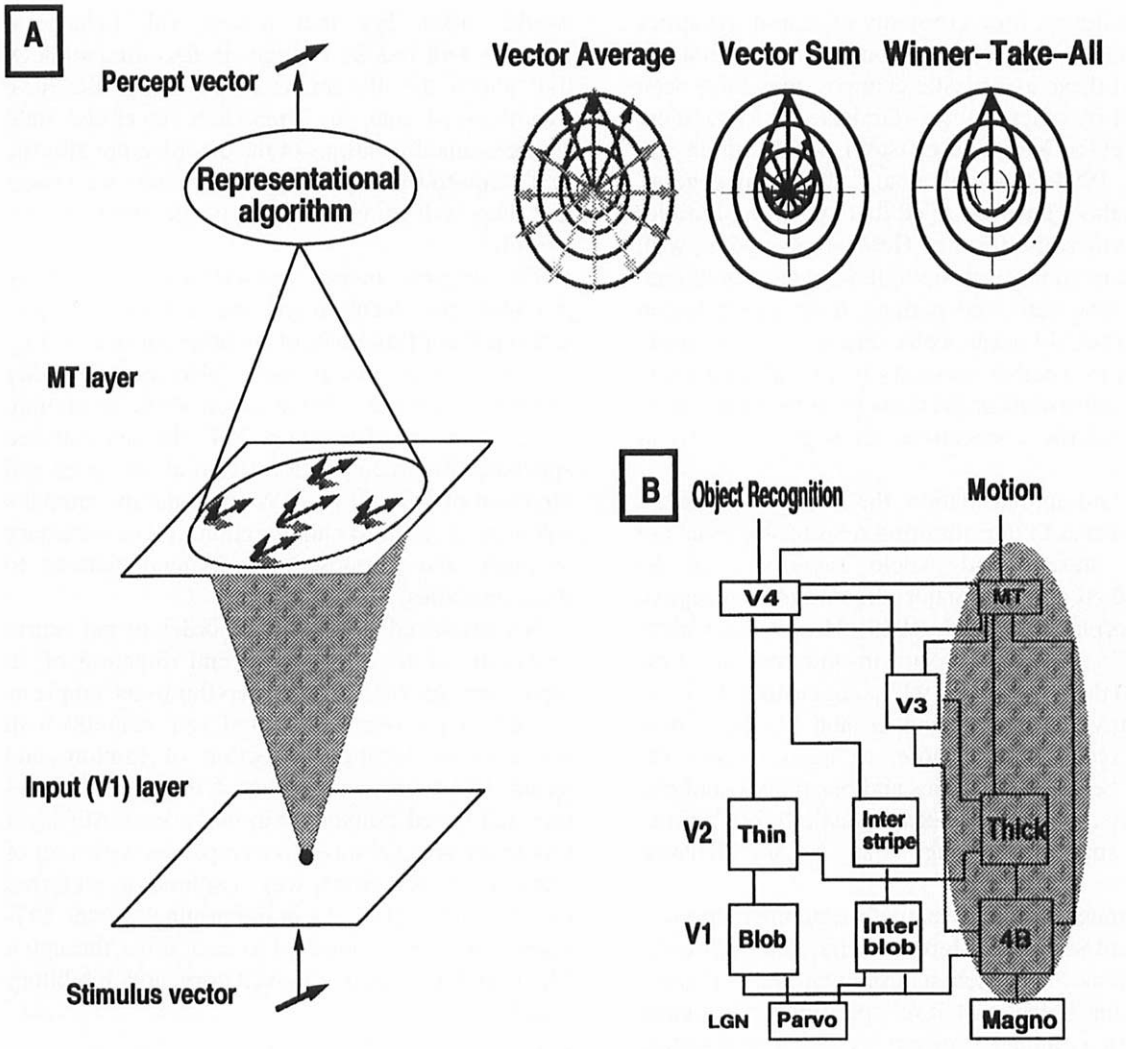

Fig. 6. (A) Estimation of the behavioral consequences of receptive field changes required a multi-level model which used an algorithm for determining the interpretation of neural activity. At the lowest level, the stimuli themselves have a speed and direction in addition to location. The next layer is a filter array with individual input units selective for location, speed, and direction. This is the 'V1 layer' or input layer. The third layer is the MT layer whose units also have velocity selectivity based on their connections from the selective units in the input layer. The final layer is the perceptual output which produces a stimulus velocity and location estimate based on the activity of individual MT units that are activated according to one of three algorithms. These three algorithms assessed are shown to the right: in vector average the preferred directions of the active vectors are weighted according to their activity and the resulting vector is then normalized to give the percept; in vector sum the same process is done, omitting the normalization; in winner-take-all the direction of the single most active vector is taken as the percept. (B) The visual system is a complex array of centers. The computer model reduces this complexity to layered two-dimensional arrays. The shaded portion of the schematic represents the motion pathway leading to area MT.

because of the simplicity; the unit with the greatest activity wins, in the sense that its direction and speed preference is taken as the direction and speed of the stimulus. This is related to the idea of local encoding, or the 'grandmother neuron', because a single neuron is able to make an identification. The two other algorithms are simple distributed representations where the information is represented

across an ensemble of neurons (Georgopoulos et al., 1982; Georgopoulos et al., 1986). In the vector sum algorithm, the magnitude of the final representation is obtained by simply adding up all of the contributions of the neurons that are firing, after weighting them in proportion to their firing rates. Hence, the representation is proportional to the number of units that contribute, with consequences for the case of stroke when this number is significantly reduced. Finally, the vector average algorithm uses a normalization step following the summation of the vectors, making the final representation independent of number of units that contribute.

RF changes predict behavioral dysfunction

In animal studies, small ablations in visual area MT cause a behavioral deficit. This can be detected by having the monkey do a visual tracking task, in which he is required to saccade to a location within the motion scotoma and then pursue the target as it moves out of the scotoma (Fig. 7A). Although a saccade to a stationary target would be accurate, the initial saccade in this task is incorrect, because the target starts moving as soon as it appears. If the target is moving away from fovea, the saccade is hypometric, and if the target is moving towards fovea, it is hypermetric, since the monkey is underestimating the velocity of the target. Furthermore, when the eyes start to pursue the object, they fall progressively behind. The location of these two symptoms of the motion scotoma, the error in initial saccade and too-slow pursuit speed, corresponds to the visual field subserved by the combined receptive fields of the ablated cells. With small ablations, this is only an area of motion obscuration, not the complete motion blindness that has been reported clinically in human stroke. Therefore, the eye pursues the stimulus in the right direction. The only evidence of deficit is that the eye does not keep up with the stimulus, the speed is underestimated and the eye falls behind. Once the target is no longer in the scotoma, the eye quickly saccades to catch up and then pursues at the proper rate thereafter.

We were able to produce the underestimation of object speed characteristic of the behavioral scotoma using either the vector average or vector summation algorithm (Fig. 7B). Using vector summation, speed estimation was reduced in the area of the scotoma due to the absence of neurons voting for the proper direction and speed. The underestimation was particularly marked in the case of vector sum because the overall strength of the sum was reduced simply by virtue of fewer vectors being added in. In the original model without the disinhibitory halo, this would produce speed underestimation even outside the area of the scotoma, due to the lack of response from neurons that were previously activated via divergence. This halo of underestimation could, however, be largely compensated by the addition of the disinhibitory halo, which tended to increase the overall vector sum, restoring the sum to that normally seen. By contrast, vector averaging was not susceptible to this surround effect since the overall signal strength was restored by the normalization process. The vector averaging algorithm produced speed underestimation within the scotoma, since disinhibited units on the lesion periphery still contributed their 'velocity votes' – many of which were in different or even opposite directions compared to the true stimulus – to a sum that was then normalized. The winner-take-all algorithm, on the other hand, did not generally produce any scotoma since the neuron that was most strongly activated still tended to be a neuron with the correct speed and direction tuning.

Although inconclusive with respect to behavioral data, the three algorithms assessed do make different predictions regarding the expected deficit. Winner-take-all suggests that the deficit would be minimal or absent. Vector sum makes the opposite prediction; the field of behavioral deficit should be larger than the field of physiological deficit. Vector average implies that the behavioral and physiological deficit zone should match. It should be noted that these algorithms are all highly simplified and are by no means mutually exclusive. Therefore, the observed speed underestimation within the scotoma, being relatively mild, could be evidence of a change in the emphasis accorded various complementary decoding algorithms. Given the ability of winner-take-all to preserve perception in this situation, more attention might be paid to a single highly active neuron under these circum-

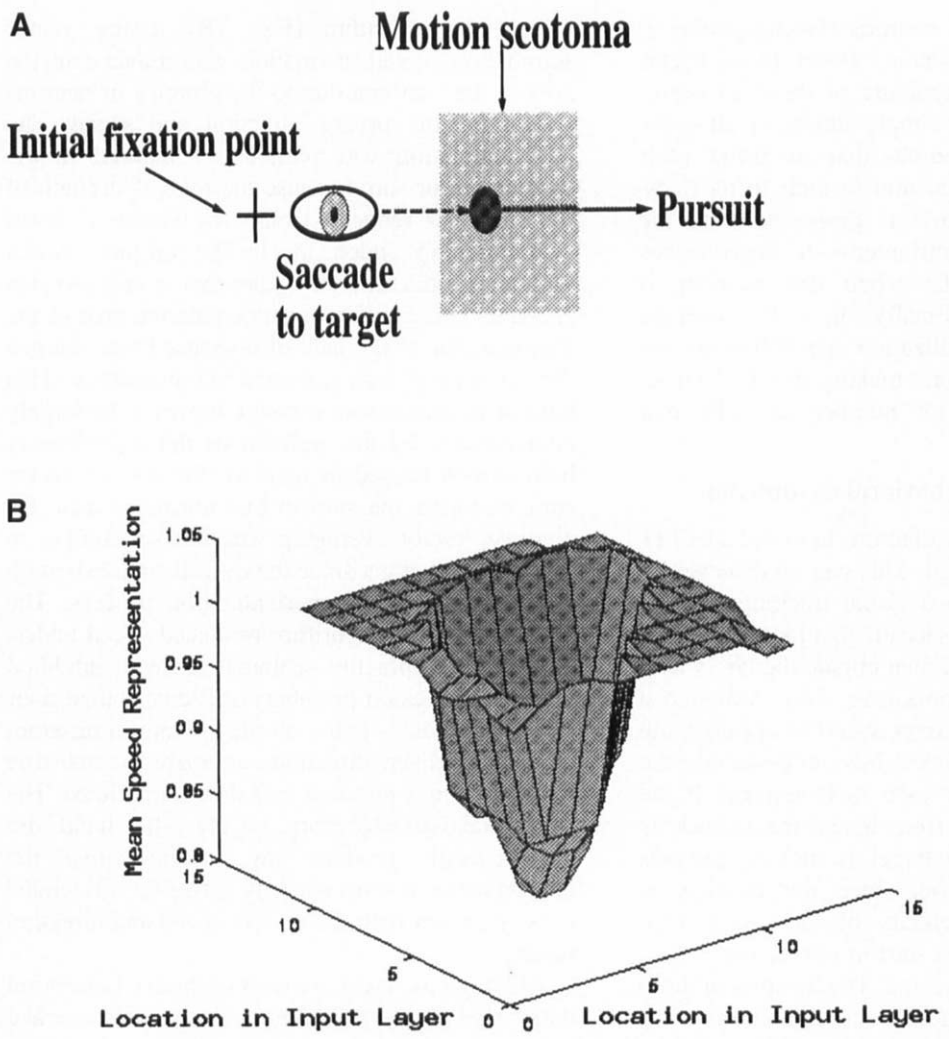

Fig. 7. (A) The pursuit task starts with the eye pointed at a central fixation point. The target comes on somewhere off to the side and immediately starts moving. The animal is expected to saccade to the target and then follow it with pursuit eye movement. The saccade itself is generally unimpaired by the MT lesion since other visual areas, both cortical and subcortical, signal the location of the target as it appears. However, the MT lesion results in some impairment in determining the velocity of the target, causing the pursuit eye movement to lag behind. This behavior suggests a perceptual deficit; the animal is underestimating velocity. (B) This velocity underestimation can be demonstrated by the model which shows different degrees of underestimation depending on the location of the target in the retinotopic zone of the lesioned area. The underestimation also depends on the representational algorithm used (see text). This case illustrates results using the vector average algorithm.

stances. This would represent an alteration in decoding strategy, as the brain learns to read the output of the damaged area differently than it did previously.

Other alterations in decoding strategy might be less drastic. For example, if a vector sum algorithm is being used, then a new decoding strategy would involve reweighting inputs from the damaged area. Compensation would require an increase in all surviving weights, in order to reestablish magnitude to compensate for the lost input. Alternatively, taking a Bayesian viewpoint, any new decoding would involve reassigning of probability distributions and prior probabilities. As a simple example,

the ablated cells would be assigned a zero probability of firing, and conditional probabilities associated with their not firing would be eliminated.

As noted above, the receptive fields of cells surrounding the lesion expand dramatically following cortical ablation; this expansion is often asymmetric with greater expansion towards the lesion. Our model suggests that this expansion plays an important role in the continued perception of speed and direction in the center of an ablation. The enlarged receptive fields effectively saved part of the input space that would otherwise entirely lose its representation in cortex. In essence, these enlarged receptive fields provided a band-aid over the area of input space that had been processed by the neurons killed by the lesion.

In the absence of these expansions, a portion of visual space would lose its cortical representation entirely because it would not fall in the receptive fields of any live neurons. The behavioral deficits that follow cortical lesion certainly suggest that such damage disrupts the brain's ability to process stimuli. Nevertheless, it is quite significant that for moderate-sized lesions this inability is reflected as an inappropriate response to stimuli rather than a complete lack of response (Yamasaki and Wurtz, 1991). Perhaps the receptive field band-aid makes a critical difference in that it allows postlesion stimuli to be misprocessed (as evidenced by inappropriate postlesion behavior) rather than not processed at all. This erroneous processing can then be corrected by Hebbian plasticity (Hebb, 1949). In general, neural network learning algorithms are good at rewiring networks that respond inappropriately, using the error to move the network towards greater accuracy. In the absence of any response, however, it is impossible to generate the correct error signal needed to move the network in the proper direction. This suggests that large lesions that destroy large tracts of cortex exceeding the typical divergence of projecting cells will be qualitatively different in their ability to recover functionally.

Changes in directional receptive fields

The behavioral model's estimation of direction following an ablation was also strongly affected by the amount of interaction between directionally tuned units in the MT layer. In the absence of substantial surround inhibition influencing direction cells, direction tuning was substantially the same both before and after the lesion. In this case, direction cell response was determined mainly by the properties of feedforward stimulation, and was not sculpted by lateral interactions within the MT layer. Using the vector summation algorithm, stimulus speed estimation is dependent on the number of summed vectors, but using the vector average algorithm, it is not. In the absence of change in direction tuning of the individual direction cells, the smaller number of cells postlesion gave a reduction in speed estimation when using the vector sum algorithm but no alteration in speed estimation with the vector-average algorithm.

By contrast, in the presence of substantial surround inhibition influencing direction tuning, direction tuning loosened after the lesion, meaning that a particular unit would respond to a wider range of directions. This was caused by the same mechanisms that caused spatial tuning loosening (spatial receptive field expansion) in the basic model. In the behavioral model, directional-selectivity inputs drove each MT unit for a certain range of directional input, just as spatial-selectivity units drove each MT unit for a certain spatial range. As in the spatial case, the actual directional tuning of an MT unit was narrower than that specified by this function because of lateral inhibition from other MT units. Lesions to the MT layer loosened MT unit tuning (that is, made tuning more similar to the driving function) by eliminating lateral inhibition. Also analogously, the inhibition was reduced both by the removal of cells with inhibitory connections and by the loss of inhibitory interneurons in the disinhibitory halo.

With lateral inhibition in place the ablation resulted in expansion of directional tuning curves as well as a reduction in the number of units. Now, both the summation and averaging of algorithms predicted speed underestimation. In the case of vector summation, this happened for the same reason as in the no-lateral-inhibition case – there are simply fewer vectors being summed, and the result is a shorter vector. In the case of vector averaging, the expansion of the directional tuning

curve introduced omnidirectional noise into the set of vectors to be averaged. Once averaged in with the signal components, these noise components, which in some cases pointed in the wrong direction, reduced the magnitude of the final output vector.

Therapeutic implications

In addition to physical rehabilitation strategies, new possibilities are emerging for pharmacological and surgical therapies. Computer modeling of the processes underlying recovery will be particularly useful in making the connection between the cellular and molecular level of these interventions and the behavioral level. Overall, the interventions that have been proposed can be classified as follows: (1) alteration of cellular dynamics; (2) alteration of activity-dependent plasticity; and (3) replacement of neurons or augmentation of existing neurons (i.e. nerve growth factors). Gross network dynamics is addressed in this paper, but the complexities of single neuron dynamics are not explored. Activity-dependent plasticity has been considered in a number of recent papers (Pearson et al., 1987; Grajski and Merzenich, 1990; Reggia et al., 1992; Cho and Reggia, 1994; Sutton et al., 1994; Xing and Gerstein, 1996). The role of sprouting or cellular replacement remains more difficult to predict at present but will also be amenable to modeling as more facts emerge.

In this paper, we have discussed how dynamics provides an initial band-aid effect that may provide immediate coverage which minimizes the disability in the short-term. As noted, this will also set up the patterned activity needed for activity-dependent plasticity changes. This increased receptive field size is likely to correlate with increased activity levels, putting this putative benefit squarely at odds with the need to reduce activity levels after stroke in order to prevent excitotoxicity due to calcium entry. One method proposed to counteract excitotoxicity is NMDA blockade, which will of course have a direct effect on activity-dependent plasticity.

Optimization of desirable activity-dependent plastic changes will require not only evaluation of the amount of activity during stroke recovery, but also consideration of the best timing for plasticity. To take an obvious example, it may be preferable to enhance plasticity during periods of active physical rehabilitation and perhaps suppress plasticity during the immediate post-stroke period when patients are inactive. There remains controversy regarding the nature of the plasticity rules governing stroke recovery, with some evidence suggesting that these rules might differ somewhat from those of development.

Neuron transplants have recently been pioneered in humans who have suffered strokes (Bonn, 1998). It is unknown whether these neurons may eventually intercalate directly into processing circuits or simply provide growth factors that produce new connections in remaining indigenous neurons. In the latter case, this procedure may have the same effect as direct administration of nerve growth factors. It is unclear whether sprouting due to these factors will be activity dependent or not. If it is activity-dependent, it is not known whether it will be governed by rules appropriate for the limited neural plasticity of adult learning or by the rules utilized in childhood for the much more substantial alterations of early development. If the latter, perhaps the process has a critical period comparable to that of early brain development.

Conclusions

Computer modeling nicely complements the ecumenical spirit of pathophysiological investigation common to neurology and psychiatry. In both of these areas, as to a lesser extent in internal medicine, the complexities of disease causation and expression require that the physician simultaneously assume various perspectives, including cellular, chemical, neural and behavioral, when assessing a patient. He or she must then estimate how the intersection of these influences is leading to worsening disease or to recovery. Similarly, computer modeling, although not having to venture into such medical arcana as HMO reimbursement policies, explores the intersections of biological and behavioral processes at vastly different scales. In the current studies, we have looked at interactions of cellular and network dynamics and considered their effects on behavior as well as the

effects that behavior will have on dynamics in turn. We have shown how the limitations of the original model suggested further investigations which revealed an unexpected histological finding—the disinhibitory halo. We have also provided some explanations, although not yet testable predictions, at the behavioral level. Our model suggests a value to neural overactivation in the immediate post-stroke period: associated expanding receptive fields may provide a band-aid effect and encourage plasticity leading to continuing recovery. This would suggest that pharmacological reduction of excitation to prevent excitotoxicity might best be restricted to a limited period immediately after a stroke.

Appendix

MT and V1 were represented by two 20×20 grids of nodes with edge wrap arround. Activity (a_k) of MT unit k was defined by

$$da_k/dt = -a_k \cdot \tau + \phi(a_k)\left(\sum_{j=1}^{400} V_{kj} b_j + \sum_{i=1}^{400} M_{ki} a_i\right) \tag{1a}$$

$$\phi(a_k) = -4(a_k^2/A - a_k) \tag{1b}$$

with $\tau = 0.2$ and $A = 5$. The V weight matrix was the projection from V1 to MT, b_j were inputs from V1, and the M weight matrix expressed lateral connectivity within MT. Function $\phi(a_k)$ was used to eliminate drive when unit activity approached 0 or A, thereby keeping a_k within these bounds.

Connections from V1 to MT were topographic with wrap-around to prevent edge effects. The elements of matrix V were excitatory (positive) and calculated from radial coordinates r of the hexagonally tessellated units as distance from target unit. Divergence from a given V1 location to the MT units had Gaussian spatial fall-off

$$V(r) = k \cdot e^{-1/2(r/s)^2} \tag{2}$$

where $k = 1.0$ is the normalizing constant and $s = 3.0$ is the divergence parameter.

Similarly, M was calculated from excitatory $E(r)$ and inhibitory $I(r)$ functions with wrap-around in the MT layer. Lateral MT excitatory connections were highly divergent and declined in strength exponentially:

$$E(r) = c \cdot e^{-r/\lambda} \tag{3}$$

with $c = 0.02$, $\lambda = 0.8$, $r \geq 1$ (no self connection).

Lateral inhibition in the model was modeled as a reduction in negative connection strength onto local MT units.

$$I(r) = c \cdot e^{-(r-1)/\lambda} \tag{4}$$

with $c = 0.0157$, $\lambda = 1.5$, $r \geq 2$. These combine by $E(r) - I(r)$ to form the 'Mexican Hat' shape.

Receptive fields were calculated by serially activating each of the 400 inputs and recording whether a given MT unit responded above threshold ($\theta = 0.5$). For simple ablations, units were eliminated from the model by locking their states at zero. For disinhibitory halo ablations, this lesion was surrounded by a zone in which inhibitory connections were reduced by 50%.

References

Alamancos, M. and Borrel, J. (1995). Functional recovery of forelimb response capacity after forelimb primary motor cortex damage in the rat is due to the reorganization of adjacent areas of cortex. *Neuroscience*, 68: 793–805.

Allard, T., Clark, S., Jenkins, W. and Merzenich, M. (1991). Reorganization of somatosensory area 3b representations in adult owl monkeys after digital syndactyly. *J. Neurophysiol.*, 68: 1048–1058.

Armentrout, S., Reggia, J. and Weinrich, M. (1994). A neural model of cortical map reorganization following a focal lesion. *Art. Intell. Medicine*, 6: 383–400.

Bonn, D. (1988). First cell transplant aimed to reverse stroke damage. *Lancet*, 352(9122): 119.

Buonomano, D. and Merzenich, M. (1998). Cortical plasticity: from synapses to maps. *Annu. Rev. Neurosci.*, 21: 149–186.

Cho, S. and Reggia, J. (1994). Map formation in proprioceptive cortex. *Int. J. Neural Systems*, 5: 87–101.

Clark, S., Allard, T., Jenkins, W. and Merzenich, M. (1988). Receptive fields in the body-surface map in adult cortex defined by temporally correlated inputs. *Nature*, 332: 444–445.

Dinse, H., REcanzone, G. and Merzenich, M. (1990). Direct observation of neural assemblies during neocortical representation reorganization. In: R. Eckmiller, G. Hartmann and G. Huske (Eds.), *Parallel Processing in Neural Systems and Computers*, Elsevier, New York, pp. 1–21.

Fisher, S., Fisher, T. and Carew, T. (1997). Multiple overlapping processes underlying short-term synaptic enhancement. *Trends Neurosci.*, 20(4): 170–177.

Georgopoulos, A., Kalaska, J., Caminiti, R. and Massey, J. (1982). On the relations between the direction of two-

dimensional arm movements and cell discharge in primate motor cortex. *J. Neurosci.*, 2: 1527–1537.

Geogopoulos, A., Schwartz, A. and Kettner, R. (1986). Neuronal population coding of movement direction. *Science*, 233: 1416–1419.

Gilber, C. and Wiesel, T. (1992). Receptive field dynamics in adult primary visual cortex. *Nature*, 356: 150–152.

Goodall, S., Reggia, J., Chen, Y., Ruppin, E. and Whitney, C. (1997). A computational model of acute focal cortical lesions. *Stroke*, 28: 101–109.

Grajski, K. and Merzenich, M. (1990). Hebb-type dynamics is sufficient to account for the inverse magnification rule in cortical somatotopy. *Neural Comp.*, 2: 71–84.

Grajski, K. and Mercenich, M. (1990) Neural network simulation of somatosensory representational plasticity. In: D.S. Taratzky (Ed.), *Adv. Neur. Inform. Process. 2*. Morgan Kaufman: San Mateo, CA.

Hebb, D., *Organization of Behavior.* John Wiley & Sons: New York, 1949.

Hubel, D. (1996). A big step along the visual pathway [news; comment]. *Nature*, 380: 197–198.

Hubel, D. and Wiesel, T. (1998). Early exploration of the visual cortex. *Neuron.*, 20: 401–412.

Kaas, J., Krubitzer, L., Chino, Y., Langston, A., Polley, E. and Blair, N. (1990). Reorganization of retinotopic cortical maps in adult mammals after lesions of the retina. *Science*, 248: 229–231.

Lytton, W., Stark, J., Yamasaki, D. and Sober, S. (1999). Computer models of stroke recovery: Implications for neurorehabilitation. *The Neuroscientist*, 5: 100–111.

Merzenich, M. and Kaas, J. (1982). Reorganization of mammalian somatosensory cortex following peripheral nerve injury. *Trends Neurosci.*, 5: 434–436.

Miller, K. (1994). Models of activity-dependent neural development. *Prog. Brain Res.*, 102: 303–318.

Miller, K. (1995). Receptive fields and maps in the visual cortex: Models of ocular dominance and orientation columns. In: van Hemmen, J. and K.S. (Eds.), *Models of Neural Networks III.* Springer Verlag: NY, Ch. 1, pp. 55–78.

Miller, K., Keller, J. and Stryker, M. (1989). Ocular dominance column development: analysis and simulation. *Science*, 245: 605–615.

Nudo, R., Jenkins, W. and Merzenich, M. (1990). Repetitive microstimulation alters the cortical representation of movements in adult rats. *Somatosens. Mot. Res.*, 7: 463–483.

Nudo, R., and Milliken, G. (1996). Reorganization of movement representations in primary motor cortex following focal ischemic infarcts in adult squirrel monkeys. *J. Neurophysiol.* 75: 2144–2149.

Nudo, R., Wise, B., Fuentes, F. and Milliken, G. (1996). Neural substrates for the effects of rehabilitative training on motor recovery after ischemic infarct. *Science*, 272: 1791–1794.

Oram, M., Foldiak, P., Perrett, D. and Sengpiel, F. (1998). The 'ideal humunculus': decoding neural population signals. *Trends Neurosci.*, 21: 259–265.

Pearson, J., Finkel, L. and Edelman, G. (1987). Plasticity in the organization of adult cerebral cortical maps: a computer simulation based on neuronal group selection. *J. Neurosci.*, 7: 4209–4223.

Recanzone, G., Jenkins, W., Hradek, G. and Merzenich, M. (1992). Progressive improvement in discriminative abilities in adult owl monkeys performing a tactile frequency discrimination task. *J. Neurophysiol.*, 67: 1015–1030.

Reggia, J., D'Autrechy, C., Sutton, G. and Weinrich, M. (1992). A competitive distribution theory of neocortical dynamics. *Neural Comp.*, 4: 287–317.

Robertson, D. and Irvine, D. (1989). Plasticity of frequency organization in auditory cortex of guinea pigs with partial unilateral deafness. *J. Comp. Neurol.*, 282: 456–471.

Sejnowski, T., Koch, C. and Churchland, P. (1988). Computational neuroscience. *Science*, 241: 1299–1306.

Smits, E., Gordon, D., Witte, S., Rasmusson, D. and Zarzecki, P. (1991). Synaptic potentials evoked by convergent somatosensory and corticocortical inputs in raccoon somatosensory cortex: substrates for plasticity. *J. Neurophysiol.*, 66: 688–695.

Sober, S., Stark, J., Yamasaki, D. and Lytton, W. (1997). Receptive field changes following stroke-like cortical ablation: a role for activation dynamics. *J. Neurophysiol.*, 78: 3438–3443.

Sutton, G., Reggia, J., Armentrout, S. and D'Autrechy, C. (1994). Cortical map reorganization as a competitive process. *Neural Comp.*, 6: 1–13.

Wang, X., Merzenich, M., Sameshima, K. and Jenkins, W. (1995). Remodelling of hand representation in adult cortex determined by timing of tactile stimulation. *Nature*, 378: 71–75.

Weinberger, N., Javid, R. and Lepan, B. (1993). Long-term retention of learning-induced receptive-field plasticity in the auditory cortex. *Proc. Nat. Acad. Sci. USA*, 90: 2394–2398.

Wurtz, R., Yamasaki, D., Duffy, C. and Roy, J. (1990). Functional specialization for visual motion processing in primate cerebral cortex. *Cold Spring Harbor Symposia on Quantitative Biology*, 5: 717–727.

Xing, J. and Gerstein, G. (1994). Simulation of dynamic receptive fields in primary visual cortex. *Vision Res.*, 34: 1901–1911.

Xing, J. and Gerstein, G. (1996). Networks with lateral connectivity I. *J. Neurophysiol.*, 75: 184–199.

Yamasaki, D. and Wurtz, R. (1991). Recovery of function after lesions in the superior temporal sulcus in the monkey. *J. Neurophysiol.*, 66: 651–673.